VLSI Device Models for Analog Circuits

Michael D. Godfrey* and John Lazzaro**

Table of Contents

 * ISL, Electrical Engineering Department, Stanford University
** CS Division, University of California at Berkeley

Abstract

This paper presents a new formulation of a CMOS device model. The model is primarily intended for analog circuit analysis. Exponential (subthreshold) and square-law (above threshold) behavior is modeled, with a smooth and accurate threshold transition. The new formulation is based on three independent physical process parameters: N_a — bulk doping concentration, Q_{ss} — fixed oxide charge, and μ_0 — effective carrier mobility. The mutual independence greatly simplifies the use of the model for prediciton and for understanding the significance of process changes. This contrasts with the present standard practise of using, for example, the threshold voltage, V_t, as a model parameter. A change in V_t must be due to a change in the flatband voltage, which depends on C_{ox}, or the Fermi potential. Changes to these parameters in turn may imply changes in the value of other model parameters such as β or γ. Thus, it is not generally consistent to change V_t while holding β or γ constant.

The model has a simple closed form and therefore is well-suited to circuit simulation. Its incorporation into the *anaLOG* circuit simulator is described. Finally, two examples of the use of the model for devices from a $1.2um$ and a $0.8um$ process are given.

In the course of reviewing the theoretical and empirical origins of the parameters for the standard device models, some anomalies were uncovered. These are discussed, and more accurate parameter values are derived. Some of these more accurate values would likely be useful in other models. By far the most important inaccuracy is the accepted value of the intrinsic carrier concentration in silicon. The widely acepted value (as uniformly used in SPICE models, for example) of (n_i) is 1.45×10^{10} at 300° K. The accurately measured value is 0.99976×10^{10}. In a typical case, this 45% error in n_i from its correct value changes V_t from 0.602 to 0.623. A $200mv$ change in V_t can have a significant effect on the behavior of many analog circuits. The accurate value of n_i has been known by people working on CCD's and by people developing silicon-based solar cells, however the information has not been noticed by the mainstream of CMOS research and design. Quite a lot of time has been spent making "adjustments" for the resulting mismatch between "theory" and observation of device behavior.

1. Introduction

At present many analog VLSI circuits contain devices operating in the subthreshold regime. There are many reasons for this, but it seems evident that technology, circuit complexity, minimum power, and performance requirements will tend to increase the use of subthreshold operation. Thus, it is important to develop models of device behavior that are suitable for modeling such circuits. A substantial amount of new work in this area has been reported in recent years [1, 2].

The purpose of this paper is to present a simple, but general and reasonably accurate model which has been incorporated in a convenient analog circuit simulator. The model is based on the mathematical approximation first introduced by Vittoz and Oguey [3]. It also continues the spirit of this elegant approximation: find simple but powerful approximations which permit the computation of device behavior from physical properties. This approach cannot accurately reflect all the details of specific technologies nor the effects of details of device construction. The objective is only to provide accuracy comparable to the variation between devices within a circuit. Thus, accuracy of about 15% is our target. More important, we intend to provide *predictive* power: to the extent possible we use only information which is readily and accurately available for the chosen process. In addition, we have incorporated the temperature dependence of all parameters. This is particularly important for analog circuits which include devices operating in the subthreshold regime.

The key property of the Vittoz-Oguey approximation is that it provides square-law behavior for large values of its argument and exponential behavior for small values. Thus, if the argument is an appropriate function of gate voltage, the suitably scaled result is source-drain current. The transition from exponential to square-law behavior is continuous and the first derivative does not change sign. However, many implementations based on this approximation have failed to produce accurate performance in terms of current values, the region in which the threshold transition occurs, and subthreshold slope. In addition, temperature effects have often been treated in an incomplete way. We have tried to correct these defects while retaining a very simple form of the model, with few parameters. In this sense we expect that our model will complement the recent work of Enz, Krummenacher and Vittoz [4] who have developed a very detailed version of the original Vittoz-Oguey model.

It is also possible to modify the Vittoz-Oguey approximation so that the above threshold behavior is some power other than two. The parameter which determines

the above threshold exponent could be made a function of the device voltages. Thus, it should be possible to deal with velocity saturation. This is discussed in more detail in [5]. Finally, short channel (DIBL) effects could be introduced. This is a phenomenon of increasing importance. However, we have not pursued it here since its greater importance is for digital circuits which rely on minimum channel length devices. In most analog circuits the problems due to DIBL-induced leakage are sufficient to dictate use of longer channels. It would be very useful to be able to predict the channel length at which DIBL begins to have a significant effect. However, this does not appear to be possible at present, except in a very approximate way.

We use the standard four-terminal model. This is done since this is the general form from the standpoint of a current-voltage model. It provides the ability to model the circuit effects of well voltages which are a function of circuit variables.

In order to carry out this plan we reviewed the standard derivations of device parameters and their temperature dependence. Generally, our intent was to trace each parameter definition back to the underlying physical properties. In doing this we have found a number of inconsistencies in the literature. We tried to resolve these inconsistencies and develop more realistic values for physical and device parameters.

There are a number of geometric and physical parameters which affect device behavior. Some of these, such as oxide thickness (t_{ox}), are quite precisely defined, while others such as threshold voltage (V_t) are notoriously poorly defined and difficult to measure. Many of these parameters play a minor or indirect role in device behavior from a circuit standpoint. There are three parameters which are independent in process terms and which play key roles in our model. These are: Q_{ss}, the channel charge due to surface states, N_a, substrate doping concentration, and μ_0, carrier mobility. Thus, these are used to "adjust" the model for specific technologies and specific fabrication runs.

2. Background

The motivation for this investigation stems from three main concerns:

1. The usual parameterization of device models for device and circuit simulation causes problems due to the interdependence of the parameters. It is not physically realistic to change any one parameter without determining the change in the process technology that would produce such a change in the parameter. Then all

the other parameters which also depend on this change in the technology must be adjusted accordingly. In addition, it is quite difficult to determine the effect of a specific change in a new technology since the available parameters each depend on a number of technology parameters.

2. The predictive performance of present models is not good. It has usually been necessary to fabricate devices in any chosen technology, and extract parameters, and then fit the model to this specific technology by use of additional "adjustment" parameters. Of course, this procedure is reasonable and useful once a technology has been chosen. However, it would be useful if the model could produce fairly accurate results if only the process specifications are used. Without such predictive accuracy it is difficult to make an initial choice of technology.

3. Most models have been developed for digital applications where devices operate above threshold and therefore are not strongly temperature sensitive. This causes problems for modeling analog circuits which use subthreshold operation. In particular, the temperature dependence of subthreshold behavior has not been fully explored. In many models some parameters which are temperature dependent have been assumed to be constant.

Device and circuit models are all based on the physical properties of semiconductor materials, the dimensions of the devices, and on theoretical and empirical equations which are intended to model electrical behavior. The distinction between theoretical and empirical equations is often unclear. Most of the equations are substantially empirical.

Of all the equations, one of the most fundamental and problematic is the equation for n_i, the intrinsic carrier concentration of a semiconductor. The definition of n_i derives from the thermodynamic equilibrium of electron and hole formation, based on the fact that the energy gap is a Gibbs energy. The equilibrium equation is

$$np = N_c N_v exp(-E_g/kT)$$

where n is the electron concentration, p is the hole concentration, N_c is the number of effective states in the conduction band, N_v is the number of effective states in the valence band, and E_g is the band gap. The carrier concentration is then given by

$$n_i = (np)^{1/2}.$$

It would appear to be a simple matter to substitute values for N_c, N_v, and kT to obtain an accurate value of n_i for a specific semiconductor. The fact that this does not

work has contributed to the acceptance of quite inaccurate results. Early attempts at empirical measurements (See [6]) were, due to experimental and materials difficulties, not accurate either.

By the early 1960's a wide range of values had been reported in the device physics literature. It is unclear how these values were determined since they depend on assumptions which are not made explicit, and on numerical values of other constants (E_g and k) which were not well-established at the time. Practically all the literature since about 1967 reports the value for silicon to be $1.45 \times 10^{10} cm^{-3}$ at 300K (see for example [7, 8, 9]). As far as we can determine, this number was first reported by Grove [7] who cited the references Hall [10], Morin [11], and Morin [6]. The most relevant reference is [6]. The graph on page 34 of [6] is similar to the graph on page 96 of [7]. This graph was likely based on Fig. 13 and Equation 3 from [6]. The equation is

$$np = 1.5 \times 10^{33} exp\left(\frac{-1.21}{Tk}\right).$$

If we accept the values in use then (especially $k = 1.60 \times 10^{-19}$) and using $E_g = 1.21$ without temperature dependence (not the value 1.1 shown in Grove's Table 4.1) the equation yields $n_i = 1.4258 \times 10^{10}$ at $T = 300K$. In addition, the standard theoretical equation, $n_i = (N_c N_v exp(-qE_g/kT))^{1/2}$, and an empirical graph are shown in [12]. However, this equation seems not to have been used. None of the values given in the contemporary literature for N_c, N_v, and E_g yield a value close to 1.45×10^{10}. In particular, in the front cover of [7] and in his Table 4.1 on page 101 Grove gives values for all these parameters. If these values are used, (with the constants $k = 1.38066 \times 10^{-23}$, $q = 1.60218 \times 10^{-19}$, and $T = 300K$) the result is 0.98301×10^{10}, not the reported 1.45×10^{10}. This might seem like a missed opportunity to get an accurate answer, but the value $E_g = 1.1$ at $T = 300K$ was not widely accepted at the time, or since.

It is obvious from the exponential dependence on E_g that small changes in E_g and changes in its temperature dependence produce a large change in n_i. Morin [6] discusses E_g and its temperature dependence and cites conflicting reported values. (He also references [11], apparently forgetting that this paper dealt only with Germanium.)

Sze [8] in Appendix H reports the same values as Grove for N_c and N_v, but the value $E_g = 1.12$ for the energy gap. With these values he should have gotten $n_i = 0.66767 \times 10^{10}$, but the value given in Appendix H is, as always, 1.45×10^{10}. The derivations of the expressions for N_c and N_v depend on deductions about effective

electron and hole mass. These theoretical deductions lead to a wide range of numerical values. The most careful analysis appears to be by Anselm ([13] pp. 342-343). His analysis leads to $n_i = 5.4932 \times 10^9$ at $T = 294$, which is about ten percent lower than the measured results given below. In any case, the universal acceptance of the value $1.45 \times 10^{10} cm^{-3}$, for which there is no justification in the literature, is odd.

Apparently independently of the work related to conventional MOS circuit technology, workers developing charge-coupled devices for imaging applications have recently arrived at an accurate value of n_i. The value that they have settled on appears in Janesick [14]. This value is stated to be deduced from the standard thermodynamic equation and is 1.0×10^{10} at 300K. However, no explicit temperature dependence is given.

Recently, Sproul and Green [15] have made careful measurements of n_i over the temperature range 77K to 300K. They used these direct measurements to determine an empirical temperature dependence equation, obtained by polynomial fitting, which yields 0.99976×10^{10} at 300K. They include data from previous measurements and report estimated errors for their data.

Our only need for n_i is to obtain a reasonable temperature dependent value for $log(N_a/n_i)$, which in turn provides the value of the Fermi potential. n_i is very strongly temperature dependent since E_g is also temperature dependent and n_i is a function of $exp(-E_g/(2kT))$. In the neighborhood of 300K n_i doubles for a change of about 9 degrees, and changes by about 8.7% from 300K to 301K. A few models avoid the use of n_i altogether. The most convincing demonstration of this approach is Mead [2].

Several authors ([16] [4]) use "adjustments" of the Fermi potential in order to improve their models. This adjustment is equivalent to the use of a different value for n_i. Since the n_i value 1.45×10^{10} is in error by about 45%, such adjustments may be useful in correcting for this error. While in the past there was good justification for doubt about the accuracy of reported values of n_i, or of $log(N_a/n_i)$, we have chosen to accept the best present measurements. This value, when used in our model, provides fairly close agreement with measured device behavior, including temperature dependence.

The modeling literature introduces parameters without much discussion of their nature, the accuracy with which they are known, or how they can be measured. In particular, it is common practice not to distinguish between physical constants, technology properties, and parameters defined by empirical equations. The definition

and the measurement method can affect both the meaning and value of physical parameters. A prominent example is threshold voltage, V_t. For an extended discussion of the definitional and measurement problems of V_t see Tsividis and Masetti [16]. In our model V_t is simply an intermediate variable. It is computed from other parameters and input variables entirely for mathematical convenience.

3. Model Derivation

In this Section we review the derivation of the model based on the Vittoz-Oguey [3] equation and make use of recent measurements to develop model expressions which have some theoretical or experimental support. Since our target is a model which is useful for circuit development and simulation, we only require predictive power with an accuracy, at best, comparable to device performance variation due to process variation, either local or between fabrication runs.

3.1 The Vittoz-Oguey Equation

The Vittoz-Oguey model is based on the observation that a function which matches

$$F(x) = \begin{cases} (\frac{x}{2})^2 & x >> 0 \\ e^x & x << 0. \end{cases} \tag{3.1}$$

in both limits is:

$$F(x) = \ln^2(1 + e^{x/2}). \tag{3.2}$$

It can be seen that this function behaves like equation (3.1) by considering the two cases, $x >> 0$ and $x << 0$. For $x >> 0$,

$$F(x) \approx \ln^2(e^{x/2}) = (x/2)^2. \tag{3.3}$$

For the case $x << 0$, note that if $\epsilon << 0$, $e^\epsilon \approx 1 + \epsilon$. Therefore, $\ln(1 + \epsilon) \approx \epsilon$ and,

$$F(x) = e^x.$$

It is important to note that this equation has no physical interpretation. It contains the right qualitative behavior, but making it provide a quantitative match to fabricated devices has proved difficult (See [17] [5] [4]). A natural choice of parameters for fitting equation 3.2 is:

$$F(x) = I_a \ln^2(1 + e^{(ax+b)/2}). \tag{3.4}$$

The parameters a and b provide a linear transformation of the independent variable x and I_a provides a scale parameter for $F(x)$. Since x is the input voltage, it should be proportional to gate voltage minus threshold voltage. This has the effect of producing square law behavior above threshold (positive x) and exponential behavior below threshold (negative x).

Next we address the problem of matching this equation to the physical behavior of CMOS devices. Essentially, we replace x by the gate voltage and determine definitions of I_a, a and b in terms of device parameters. Following Vittoz and Enz ([18, 17]) we write the standard model equations in the form:[1]

- Above threshold

$$I_{f,r} = \frac{\beta}{2\kappa}(V_g - V_{t0} - \frac{1}{\kappa}V_{s,d})^2 \tag{3.5}$$

  where $I_{f,r}$ is the forward (f) current due to V_s or reverse (r) current due to V_d, $\beta = \mu C_{ox}W/L$ where μ is mobility, C_{ox} is oxide capacitance, and W/L is the width to length ratio of the device, $\kappa = C_{ox}/(C_{ox} + C_{dep})$ where C_{dep} is the depletion capacitance (Inmany presentations κ is not included explicit in the scale coefficient – it is typically assumed to be constant and close to one in above threshold.), V_g is the gate voltage, $V_{d,s}$ is the drain (d) or source (s) voltage, and V_{t0} is the threshold voltage. Threshold voltage has many definitions as discussed in detail by Tsivitis and Masetti [16]. We use the definition derived by Vittoz in [19, 4] except that we do not include his "adjustment factor" called "a few U_t." This adjustment factor appears only to be needed to bias the value of V_{t0} so that better results are obtained when using the Enz, Krummenacher, Vittoz (EKV) model [4].

- Below threshold

$$I_{f,r} = K_w \beta U_T^2 e^{\frac{1}{U_T}(\kappa(V_g - V_{t0}) - V_{s,d})} \tag{3.6}$$

  where K_w is a scale term to be defined below, and $U_T = kT/q$, where k is Boltzmann's constant, T is temperature, and q is the electron charge.

The source-drain current, I_{ds}, is then given by $I_{ds} = I_f - I_r$.

The substantive problem in using equation (3.4) to approximate these equations is that K_w must be given by

$$K_w = \frac{2}{\kappa}. \tag{3.7}$$

---

[1] For simplicity we do not include the size (W/L) and channel length modulation terms. They will be included in the computational equations.

This definition yields values not far from those often used in device modeling in the above threshold regime, but requiring this value here is really a consequence of the mathematics, not the physics.

Accepting the definition of K_w given in equation (3.7), the required expressions for I_a, a and b are determined by taking the pre-exponential and exponent terms in (3.6) and equating them to the corresponding terms in

$$F(x) = I_a e^{(ax+b)}$$

and then substituting into (3.4). Thus,

$$I_a = \frac{2\beta}{\kappa} U_T^2$$

and

$$ax + b = \frac{1}{U_T}(\kappa V_g - (\kappa V_{t0} + V_{s,d})).$$

Taking $x = V_g$ we have

$$a = \frac{\kappa}{U_T},$$

and

$$b = -\frac{1}{U_T}(\kappa V_{t0} + V_{s,d}).$$

This gives the final form

$$I_{f,r} = \frac{2\beta}{\kappa} U_T^2 \left(log^2 \left(1 + e^{\frac{1}{2U_T}(\kappa(V_g - V_{t0}) - V_{s,d})} \right) \right). \tag{3.8}$$

This equation is attractive due to its simplicity, its closed form, and the small number of parameters used. However, its usefulness as a device model can only be established by experimental measurements.

3.2 The Quantitative Model in Computational Form

The equations below were derived from the *Octave* code which was used to study the device model. The actual Octave code is shown in Appendix A. (Octave is a public-domain language which is similar to Matlab. Since it is public-domain, it is more easily available, and it offers features which make it more effective than Matlab for tasks such as ours. See http://www.che.wisc.edu/pub/octave for details.) The equations are given in the order required by a sequential processing language like Octave. The Octave program was written to allow the input voltages, V_d, V_s, V_g and

V_b to be vectors. The resulting current is returned as a vector. This makes it easy to use the code to produce IV-curves. It is correspondingly easy to apply the same vectors to test equipment (we also use Matlab, driving a GPIB instrument connection, to do this) for device measurement.

In the technology parameters section, example values are given for all the parameters. These values are from a recent MOSIS run using a 1.2um N-well process.

3.3 Semiconductor Properties

The parameters used to describe semiconductor devices fall into several categories. The classification of parameters is important to understanding the nature and uses of any model. We use the following classification:

1. *Physical Constants.* These provide the quantitative information about the materials used in semiconductor device construction.

2. *Geometry and Voltages.* These are the physical dimensions of devices and the voltages applied to the terminals of the device.

3. *Technology Determined Parameters.* These are properties of devices which are determined by the processing steps used in fabrication. It is uncertainty about the values and role of these parameters which often cause problems in model formulation and use.

3.3.1 Physical Constants

Several physical constants are used in determination of properties of semiconductor devices. These are:

Physical Constants:

$$k = 1.380658 \times 10^{-23} \qquad \text{Boltzmann's const. (joule/deg. K)}$$
$$q = 1.60217733 \times 10^{-19} \qquad \text{e-charge (coulomb)}$$
$$\epsilon_v = 8.854187817 \times 10^{-12} \qquad \text{permittivity of vacuum (f/m)}$$
$$\epsilon_s = 11.7\epsilon_v \qquad \text{permittivity of Si (f/m)}$$
$$\epsilon_{ox} = 3.9\epsilon_v \qquad \text{permittivity of Si02 (f/m)}$$

The values for k, q, and ϵ_v are from [20]. The value for ϵ_s is from [8] and that for ϵ_{ox} is from [21].

3.3.2 Signal Values and Device Geometry

The required input voltages and temperature and size parameters are shown below.

Signal Values, Temperature, and Device Geometry:

- Voltages are with respect to V_s as reference.

  $\vec{V}_d, V_s, \vec{V}_g, V_b$

- Temperature and drawn dimensions.

$T = 298$	Temperature in Kelvin
$W_d = 48$	Drawn width of device in λ units
$L_d = 24$	Drawn length of device in λ units

3.3.3 Technology Parameters

Most of these parameter values are routinely measured for a process run and reported as SPICE parameter values. Many of these measurements are directly useful for our purposes. However, two critical parameters present problems:

N_a - bulk doping concentration. The value for this parameter is usually depth dependent, and the doping profile affects device behavior.

Q_{ss} - charge due to surface states in channel. Charges in the channel surface states arise from several sources [22]. Fabricators often use a channel implant step which creates a fixed charge in the channel in order to lower V_t. This is most commonly done for well devices in an N-well process. This parameter is not normally extracted or published for SPICE purposes. Since V_{fb} is a linear function of Q_{ss}, Q_{ss} shifts the threshold voltage and subthreshold current. This is why it is used as a fabrication "tuning" parameter.

The technology parameters, with example values from a 1.2um N-well process, are:

Technology parameters:

$\lambda = 0.6$ scale parameter: Model is scalable using lambda

$L = \lambda L_d - .33$ actual length(um) = drawn$\times \lambda$ - delta$-$length
$W = \lambda W_d - .49$

$t_{ox} = 216 \times 10^{-10}$ oxide thickness (SPICE TOX) (meters)

$\phi_{ms} = -0.3$ silicon-oxide interface charge (poly gate devices)
     ϕ_{ms} is positive for P-channel device

$\psi = 0.6$ potential at neutral edge of depl (SPICE L2 PHI) (V)

$Early_s = 0.12$ Early effect slope

$L_0 = 0.1$ Early effect intercept

$Q_{ss} = 5.5 \times 10^{-4}$ fixed oxide charge (also Qf: M&K pgs. 399-405)
     See discussion in Sze pg.487

$Na_L = 0.0$ effecttive doping concentration dependence on L

$N_a = 3.11 \times 10^{16} \Delta N_a (1 - Na_L L)$

     bulk doping conc (SPICE L2 NSUB) (cm^{-3})

$\Delta N_a = 1.0$ N_a adjustment term

$\mu_0 = 686.6 \Delta \mu_0$ carrier mobility (SPICE L2 u0) ($cm^2/(Vs)$) at 300K

$\Delta \mu_0 = 1.0$ μ_0 adjustment term

All of these parameters, except λ, may have different values for for N-channel and P-channel devices.

3.4 Device Model

At this point all the information required by the model has been specified. The following Sections describe the computation performed on this information.

The only parameter that is not easily obtained, for example from the SPICE data provided by MOSIS, is Q_{ss}. Q_{ss} should be available as part of the fabricator's process data. However, this is often not the case. If test transistors are available, a value that yields accurate (subthreshold) results is easily obtained. Since Q_{ss} has a very strong effect on subthreshold current, a subthreshold I-V curve can be used to compute the effective Q_{ss}. The stability of Q_{ss} between wafer runs is not well-known. This is crucial for subthreshold circuit modeling, and deserves much more attention.

The use of ΔN_a and $\Delta \mu_0$ reflects the fact that reported values for these parameters may not accurately reflect the behavior of devices from a specific wafer run. At present we do not have sufficient data to determine if there is a systematic bias between the reported values and the values that yield the most accurate model results averaged over a number of wafer runs.

3.4.1 The Preliminary Equations

First we compute some common functions of the technology parameters. These functions are widely used in device modeling and provide a notational and computational convenience.

Common functions of the technology parameters:

$$\rho = qN_a \qquad\qquad \text{depl charge/area } (N_a \ cm^{-3})$$
$$C_{ox} = e_{ox}/t_{ox} \qquad\qquad F/m^2$$
$$V_{fb} = \phi_{ms} - Q_{ss}/C_{ox}$$

Next, we define a number of parameters which appear in device models which are determined by empirical expressions. Some of these expressions have some theoretical basis, but their role in device behavior or their quantitative values are not well-established other than by empirical fitting of measured data. These are:

Empirical Equations:

- Temperature dependence of band gap (E_g): See Bludau (8).

  For $0K < T < 150K$: $E_g = (1.1700 + 1.059 \times 10^{-5}T - 6.05 \times 10^{-7}T^2)q$

  For $150K < T < 300K$: $E_g = (1.1785 - 9.025 \times 10^{-5}T - 3.05 \times 10^{-7}T^2)q$

- Intrinsic Carrier Concentration.
  $$n_i = 1.640 \times 10^{15}T^{1.706}exp(-E_g/(2kT)) \quad \text{(See Sproul \& Green (9).)}$$

- Temperature dependence of μ (See Sze pgs. 29-30.)

  For N-channel: $\mu = \mu_0(T/300)^{-2.42}$

  For P-channel: $\mu = \mu_0(T/300)^{-2.30}$

  $$\beta = \mu \times 10^{-4} \times C_{ox}(W/L) \qquad \mu \ (cm^2/(V*s)) \quad C_{ox} \ (F/m^2)$$
  $$U_T = kT/q$$
  $$\phi_f = U_T log(Na/n_i)$$
  $$\phi_b = 2\phi_f$$

- Channel length modulation (linear) (See Mead (2) pg. 235.):
  $$\vec{\lambda}_c = \pm Early_s \cdot /(\vec{V}_g + L - L_0)$$
  $$\vec{V}_0 = 1.0 \cdot /\vec{\lambda}_c$$

- Body effect (10^6 converts $cm^3 -> m^3$).
  $$\gamma = (1/C_{ox})(2\rho\epsilon_s 10^6)^{1/2}$$

- Threshold Voltage.
  $$V_t = V_{fb} \pm |\phi_b| \pm \gamma(|\phi_b| \mp V_{bs})^{1/2}$$

- tanh approximation for surface potential ϕ_s.

  ϕ_s approaches a minimum near $V_{fb} + V_{bs}$ and increases to asymptote

  of $2\phi_f$ above V_t
  $$\vec{\phi}_s = 2\phi_f \tanh((\vec{V}_g - (V_{fb} + V_{bs}))/V_t)$$

  $$\vec{C}_{dep} = (\rho\epsilon_s 10^6 \cdot /(2\vec{\phi}_s))^{1/2}$$

  $$\vec{\kappa} = C_{ox} \cdot /(C_{ox} + \vec{C}_{dep})$$

Most of the above equations are either simple definitions or well-established by both theory and experimental measurement. There are two that deserve some comment. First is the definition of threshold voltage. The uncertainty about threshold voltage is fully documented and is clearly summarized by Tsividis and Masetti [16]. We have chosen a definition which is most nearly consistent with the derivation of Vittoz model given in Section 3.1. Second is the equation for the surface potential, ϕ_s. The behavior of ϕ_s, particularly in subthreshold, deserves further study[2]. The form we have chosen is mainly for computational convenience: it is a simple function of voltages. Some computational experiments indicate that, for our intended modeling accuracy, this mathematical approximation produces results similar to what would be achieved with a function that approximates exponential behavior of ϕ_s in subthreshold.

3.4.2 Device Model Equations

The parameters presented above permit evaluation of the model equations as follows:

The first two equations are simply notational and provide faster computation in the Octave interpretive system. The next three equations are the core expressions that compute I_{ds}.

Intermediate equations:

$$\vec{k}_1 = 2\beta U_T^2 \cdot /\vec{\kappa}$$
$$U_1 = \pm\frac{1}{2U_T}$$

Model Equations:

$$\vec{I}_f = (log(1 + exp(U_1(\vec{\kappa} \cdot \times(\vec{V}_g - \vec{V}_t) - V_s)))).^2$$
$$\vec{I}_r = (log(1 + exp(U_1(\vec{\kappa} \cdot \times(\vec{V}_g - \vec{V}_t) - \vec{V}_d)))).^2$$
$$\vec{I}_{ds} = \vec{k}_1 \cdot \times(\vec{I}_f - \vec{I}_r) \cdot \times(1 + \vec{\lambda}_c \cdot \times\vec{V}_{ds})$$

Note that in all equations we use the Matlab and Octave convention that *log* means logarithm base *e*.

---

[2] Rahul Sarpeshkar made some useful suggestions for a more theoretically justifiable form after we had substantially completed this paper.

3.4.3 Square-law and Exponential Equations

The following equations evaluate the square-law (drift) and exponential (diffusion) models for comparison with the Vittoz-Oguey approximation. These last equations would not normally be used in circuit simulation, and are not included in the code used in anaLOG.

Computation of square-law and exponential models:

$$\vec{I}_{fsq} = (U_1(\vec{\kappa} \cdot \times max(\vec{V}_g - V_t, 0) - V_s))^{.2}$$
$$\vec{I}_{rsq} = (U_1(\vec{\kappa} \cdot \times max(\vec{V}_g - V_t, 0) - \vec{V}_d))^{.2}$$
$$\vec{Ids}_{sq} = \vec{k}_1 \cdot \times (\vec{I}_{fsq} - \vec{I}_{rsq}) \cdot \times (1 + \vec{\lambda}_c \vec{V}_{ds})$$
$$\vec{I}_{fexp} = exp((1/U_T)(\kappa \cdot \times (\vec{V}_g - V_t) - V_s))$$
$$\vec{I}_{rexp} = exp((1/U_T)(\kappa \cdot \times (\vec{V}_g - V_t) - \vec{V}_d))$$
$$\vec{Ids}_{exp} = \vec{k}_1 \cdot \times (\vec{I}_{fexp} - \vec{I}_{rexp}) \cdot \times (1 + \vec{\lambda}_c \cdot \times \vec{V}_{ds})$$

3.5 Role of Q_{ss}, $\Delta\mu_0$, and ΔN_a

Since these three parameters are important to device behavior and are used for matching measured results, it is important to trace their role in the model.

Q_{ss} appears in $V_{fb} = \phi_{ms} - Q_{ss}/C_{ox}$. Substituting for C_{ox} and ϵ_{ox} we get $V_{fb} = \phi_{ms} - 2.9 \times 10^{10} Q_{ss} t_{ox}$. For N-type devices $\phi_{ms} = -0.3$ Thus, in this case, a positive value of Q_{ss} increases V_{fb}. Typical $1.2um$ processes have a t_{ox} of about $200A^o$ and t_{ox} for $0.8um$ processes is typically about $100A^o$. Thus, for a $1.2um$ process a value of $Q_{ss} = 0.5 \times 10^{-4}$ will increase V_{fb} by ten percent. V_{fb} appears only as an additive term in the threshold voltage (V_t) equation. This is exactly why fixed charge is implanted in production: to shift the threshold voltage. And, this is what it should be used for in case measurements indicate that the model does not reflect a "correct" threshold value.

μ appears in $\beta = \mu C_{ox}(W/L)$ and β is a term in the pre-exponential constant in the final current equation. Thus, $\Delta\mu_0$ simply scales the value of I. This is the reason why it makes sense to to set $\Delta\mu_0$ so that the above threshold current matches measured data.

N_a appears in $\phi_f = U_T log(N_a/n_i)$. Therefore, ΔN_a contributes to ϕ_f by $\phi_f = U_T log(\Delta N_a) + U_T log(N_a/n_i)$. Thus, ΔN_a modifies V_t and affects the threshold transition and subthreshold behavior.

3.6 The EKV Model

The Enz, Krummenacher, and Vittoz (EKV) model is fully described in [4]. In addition, the implementation (in C) of the model is available from the authors. A large number (on the order of 50) parameters are available in order to model many behavioral effects. However, the model may also be "simplified" by assuming default values for many of these parameters. Since in the end the EKV model uses the same model equations as used above, the differences between the two are in the handling of the parameters and variables required by the basic equations:

$$\vec{I}_f = (log(1 + exp(U_1(\vec{\kappa} \cdot \times (\vec{V}_g - V_t) - V_s))))^{.2}$$
$$\vec{I}_r = (log(1 + exp(U_1(\vec{\kappa} \cdot \times (\vec{V}_g - V_t) - \vec{V}_d))))^{.2}$$
$$\vec{I}_{ds} = \vec{k}_1 \cdot \times (\vec{I}_f - \vec{I}_r) \cdot \times (1 + \lambda_c \cdot \times \vec{V}_{ds})$$

We believe that the EKV formulation can only productively be used by experts in device modeling and fabrication technology. This is due to the large number of parameters and to the fact that these parameters interact in ways that can only be understood in the context of an extensive understanding of device physics and technology.

Our formulation, on the other hand, can be used by circuit designers using only a very basic knowledge of devices and technology. The resulting circuits will need to be designed more conservatively due to the limited accuracy of the model. However, this is in any case a good, and often cost-effective, design methodology. Fabrication is not yet perfectly accurate either.

4. Model Integration into anaLOG

This Section assumes some familiarity with the anaLOG circuit simulator. anaLOG is described as part of the analog VLSI design toolset developed at Caltech. Full information about these tools can be found at:

`http://www.cs.berkeley.edu/~lazzaro/chipmunk/`

While this model uses the same basic Vittoz-Oguey approximation as was used in current anaLOG device models, the changes in parameterization, temperature dependence, and other details made the integration into anaLOG a substantial effort. The fact that several parameters which were previously constant, such as V_t, and κ, are now functions of input voltages has increased the amount of computation required

in the equation solver. However, measured execution times for the new model are only about 30% longer than the old model.

The use of anaLOG with the new model is based on several new transistor models and other objects. These are all in the anaLOG library starting with version 5.40.

New transistor models:

NFET7T Three terminal N-channel device using the model equations from this paper.

NFET7F Four terminal N-channel device using the model equations from this paper.

PFET7T Three terminal P-channel device using the model equations from this paper.

PFET7F Four terminal P-channel device using the model equations from this paper.

New parameter objects:

THERMAL Object containing the current temperature.

PHYSICAL Object containing physical constants.

DEVTECHN Object containing scale and process parameters for N-channel devices.

DEVTECHP Object containing scale and process parameters for P-channel devices.

RUNSPEC Object containing fabrication run specific adjustment terms: ΔNa, $\Delta \mu_0$, and ΔQ_{ss}.

Appendix B shows the detailed contents of each of these new objects.

5. Experimental Results

Devices from two technologies have been examined. The two processes are quite dissimilar, as will be seen. The first technology is a $1.2um$ N-well process. Each chip contains 6 well and 6 native transistors. The transistor sizes (WxL) are: 4x4, 8x8, 12x24, 12x24(V), 24x12, and 48x24, in λ units. All transistors have the same orientation except 12x24(V), which is rotated 90°. No other devices are near these transistors on the chip. The second technology is a $0.8um$ N-well process. In this case we fabricated a test array composed of N and P devices of the following sizes: 6x2, 4x8, 24x2, 4x16, 3x8, 4x4, and 4x2.

Two measurements were made for each transistor: I_{sat} vs V_{gs} with V_{ds} fixed at 5v and I_d vs V_{ds}. For the well transistors, I_{sat} was measured for a set of well-bias (V_{bs}) values. I_d was measured for a set of (subthreshold) V_{gs} values. In addition, the I_{sat} vs V_{gs} data were used to compute the transconductance, $G_m = \partial I_{sat}/\partial V_{gs}$, as a function of V_{gs}. Generally, only the I_{sat} vs V_{gs} plots were used for determination of the best values for Q_{ss}, $\Delta\mu_0$, and ΔN_a.

The procedure for investigating each of these technologies was:

1. Compare sample measurements with the model results with $Q_{ss} = 0.$ and $\Delta\mu_0 = \Delta N_a = 1.0$. These results were used to choose "reasonable" values for Q_{ss} for both native and well devices.

2. Next, a value of $\Delta\mu_0$ was chosen to cause the model to match the above threshold current values.

3. Finally, a value for ΔN_a was chosen to match the current values in subthreshold.

Comparisons of measured I_{sat} vs V_{gs} with predicted values from the model, when plotted on a log scale, tend to "look good" even when the measured values are significantly different from the predicted values. This is due to the log scale which typically has a range of about 10^8. This optimistic view is usually corrected by looking at G_m since taking first derivatives tends to make such differences more obvious. It is also important to have reasonably accurate predicted values of G_m in order to accurately model many circuits.

For each of the two processes the results for each of the three steps are shown below. The example results chosen are for 4x4λ devices (one N and one P-type) from the 1.2um process (12 chips were measured), and 6x2λ devices (one N and one P-type) from the 0.8um process (8 chips were measured). The results for the sequence of parameter adjustment steps indicate the accuracy obtainable with only (MOSIS available) process data, and with adjustments for the specific fabrication run. Note that, counting Q_{ss}, there are only 3 parameters. Each parameter represents a separate processing step in the construction of the physical device. Processing choices will affect each of these parameters separately for N-type and P-type devices. Therefore, it is reasonable to determine an N-type and a P-type value for each one separately.

For both technologies, plots are shown of I_{sat} vs. V_{gs}, and I_d vs. V_{ds} first with default settings of ΔN_a and $\Delta\mu_0$ and then with Δ values from the table above. Finally, a plot of g_m vs. V_{gs} is shown. The I_{sat} and g_m plots show the model curve (marked with +) and all data curves. The data curves cannot usefully be

distinguished on the *log* scale. For the I_d curves only three typical data curves are shown since showing more of the data made the plots too overloaded with curves, and space would not permit additional curves. For each set of three data curves each tenth point is marked: o for the first device, x for the second, and * for the third.

These plots are more usefully viewed in color using the original PDF file, or printing on a color printer.

5.1 $1.2um$ **N-well Process**

For this process the parameter values that produce good accuracy are:

	N-type	P-type
Q_{ss}	6.1×10^{-4}	1.26×10^{-4}
$\Delta\mu_0$	0.58	0.84
ΔN_a	1.0	1.0

Below we show sample results for 4λ by 4λ transistors.

5.1.1 Results for N-type Devices

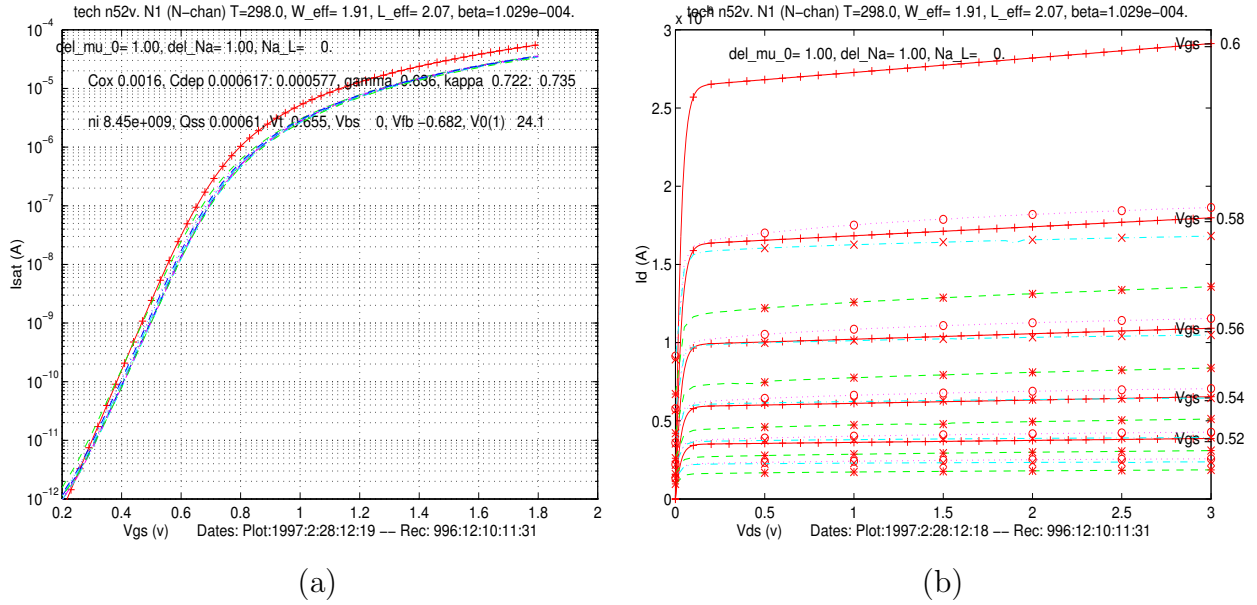Results without Δ parameter adjustment:

(a) (b)

Figure 1: Unadjusted Model and Measurements, N-channel $1.2um$.

For each Figure the solid line (with cross marks) is the model value, and the dashed lines are experimental measurements. All of these measurements were taken at approximately 25^0C. In Figure 1(a) the model curve shows close agreement in subthreshold, but overshoots by a significant amount in above threshold current values. Correspondingly, in Figure 1(b) the model currents are well above the measured values. This suggests that the reported mobility parameter is greater than is consistent with the measurements.
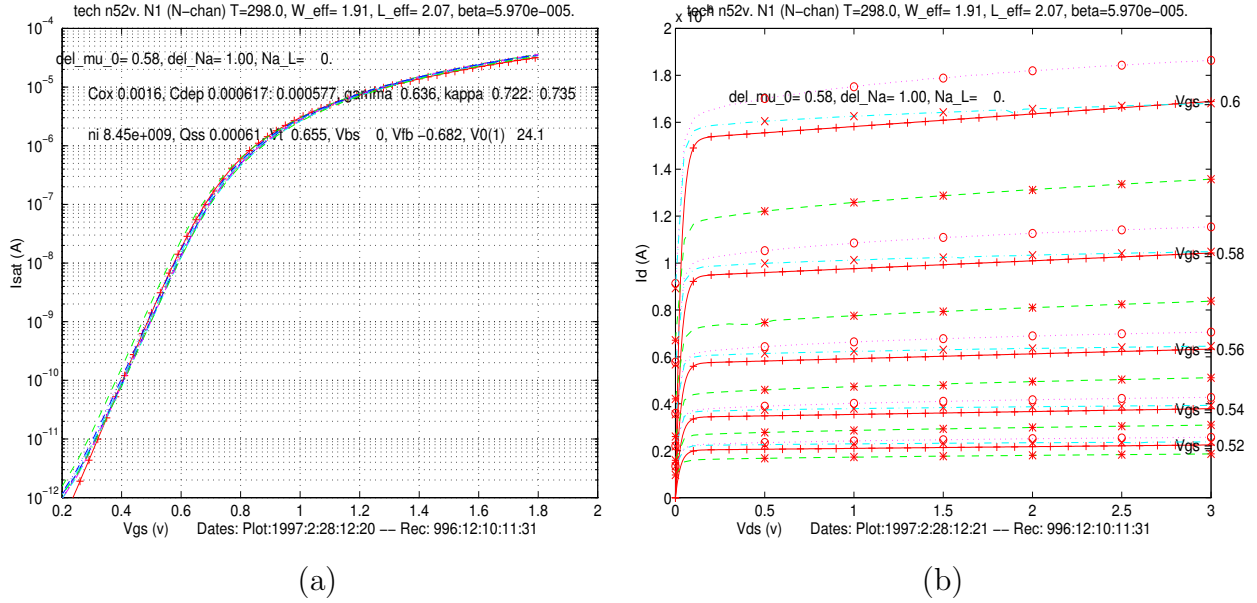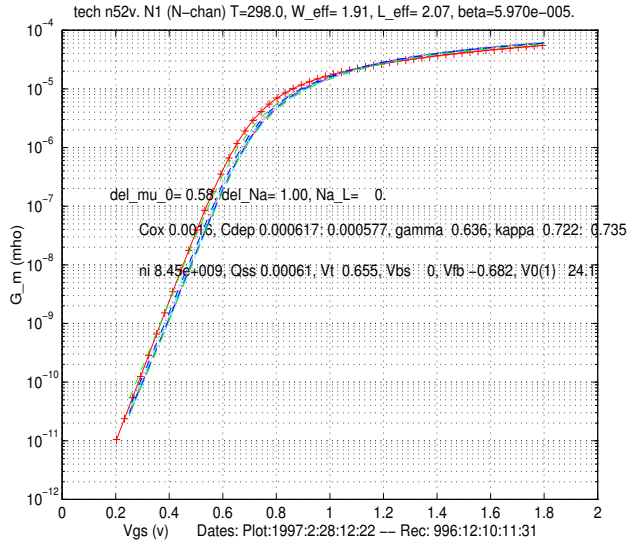
Results after $\Delta\mu_0$ adjustment:

(a)

(b)

Figure 2: Model adjusted with $\Delta\mu_0$ and Measurements, N-channel $1.2um$.

With the value $\Delta\mu_0 = .58$ the model curves and the measured values are in close agreement. It is also remarkable that the measured values have quite small variation. This appears to be a feature of many processes as of about 1995. Improving fabrication technology has led to much reduced variation within wafer runs as well as from one run to another.
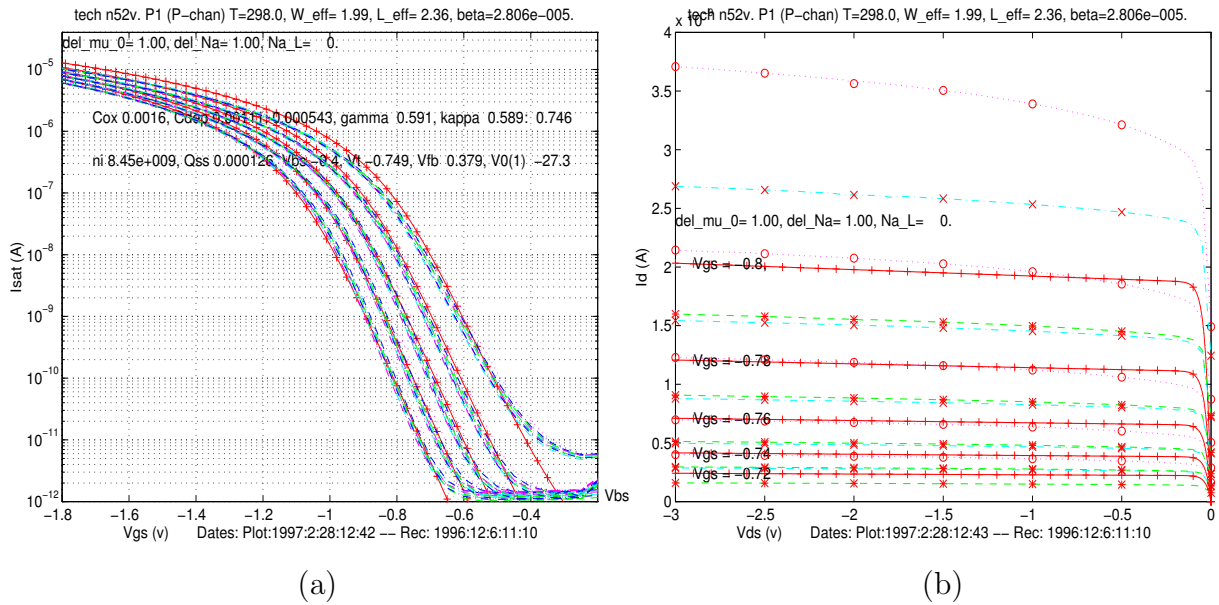
Since the final ΔN_a was 1.0, there was no additional change in the parameters.

Finally, we show a plot of g_m vs. V_{gs}:

Figure 3: g_m vs. V_{gs} Model and Measurements, N-channel $1.2um$.

5.1.2 Results for P-type Devices

Results without Δ parameter adjustment:

(a)

(b)

Figure 4: Unadjusted Model and Measurements, P-channel $1.2um$.

Results after $\Delta\mu_0$ adjustment:
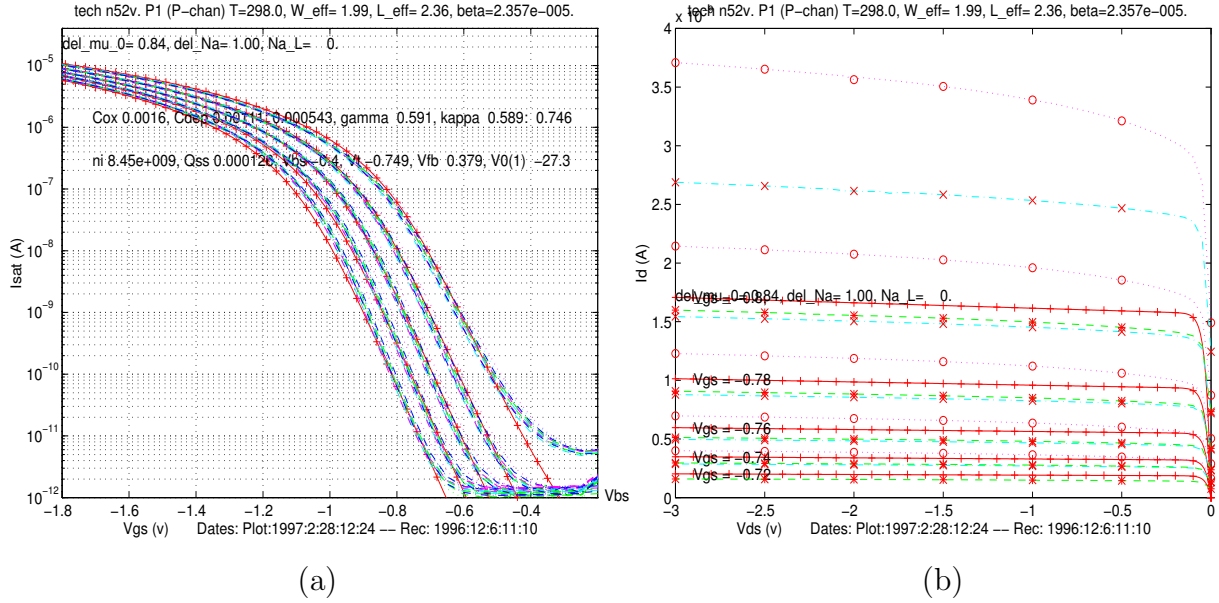

(a)   (b)

Figure 5: Model adjusted with $\Delta\mu_0$ and Measurements, P-channel $1.2um$.

Since the final ΔN_a was 1.0, there was no additional change in the parameters.
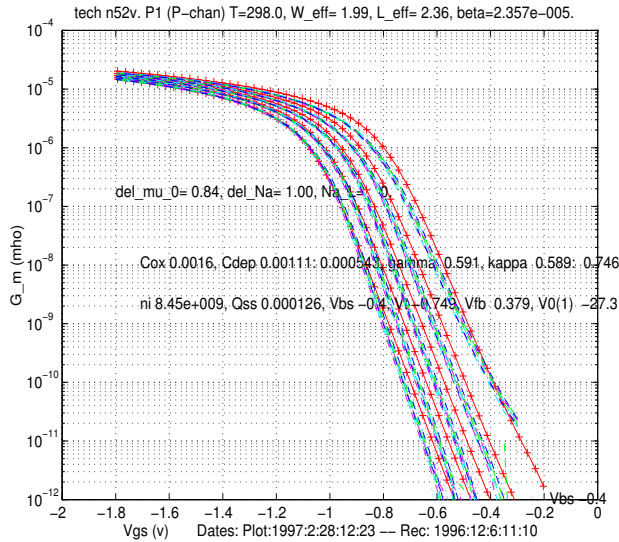
Results for g_m vs. V_{gs}:

Figure 6: g_m vs. V_{gs} Model and Measurements, P-channel $1.2um$.

5.2 $0.8um$ **N-well Process**

For this process the parameter values that produce good accuracy are:

	N-type	P-type
Q_{ss}	-5.0×10^{-4}	5.0×10^{-4}
$\Delta\mu_0$	0.55	0.75
ΔN_a	0.6	1.05

Below we show sample results for 6λ by 2λ transistors. As before, plots are shown of I_{sat} vs. V_{gs}, and I_d vs. V_{ds} first with default settings of ΔN_a and $\Delta\mu_0$ and then with Δ values from the table above. Finally, a plot of g_m vs. V_{gs} is shown.

5.2.1 Results for N-type Devices

Results without Δ parameter adjustment:

(a)   (b)

Figure 7: Unadjusted Model and Measurements, N-channel $0.8um$.

Results after $\Delta\mu_0$ adjustment:

(a)

(b)

Figure 8: Model adjusted with $\Delta\mu_0$ and Measurements, N-channel $0.8um$.

Results after ΔNa adjustment:

(a)   (b)

Figure 9: Model adjusted with $\Delta\mu_0$ and ΔNa and Measurements, N-channel $0.8um$.

Results for g_m vs. V_{gs}:

Figure 10: g_m vs. V_{gs} Model and Measurements, N-channel $0.8um$.

5.2.2 Results for P-type Devices
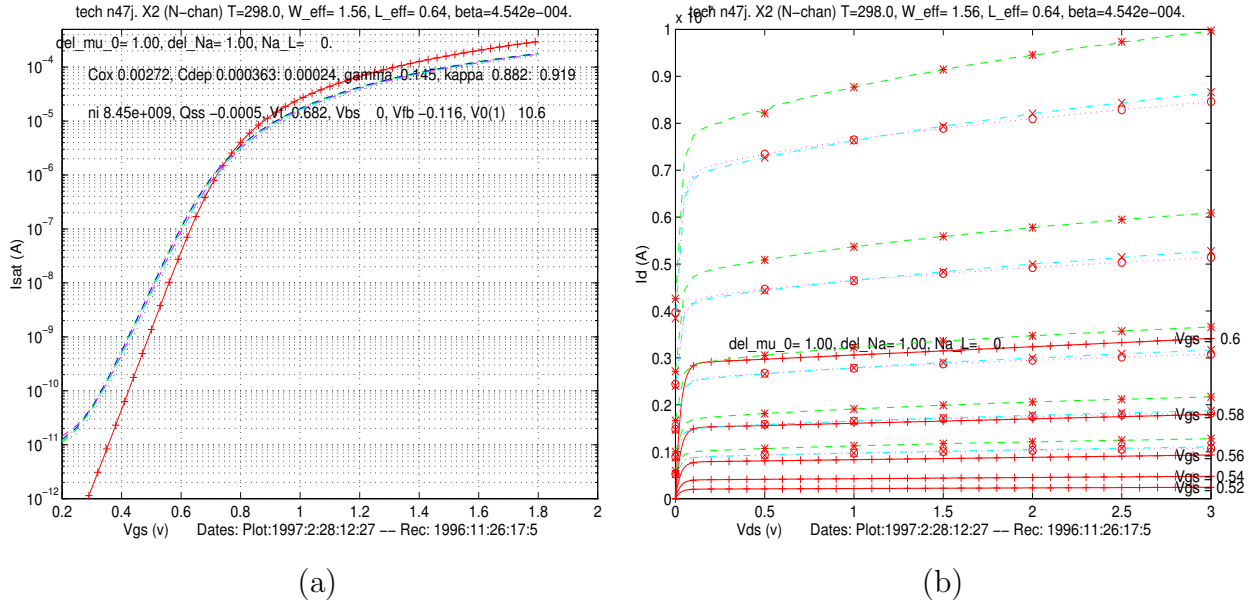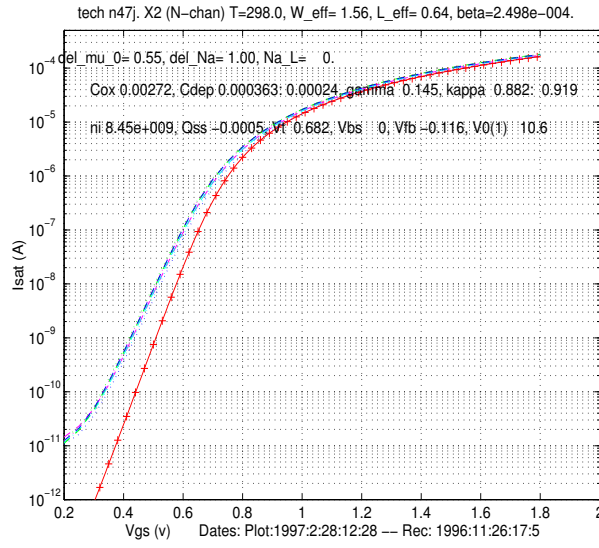
Results without Δ parameter adjustment:
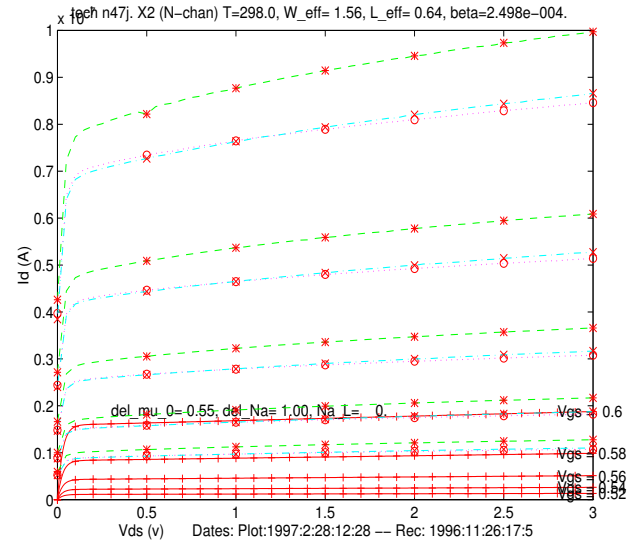

Figure 11: Unadjusted Model and Measurements, P-channel $0.8um$.

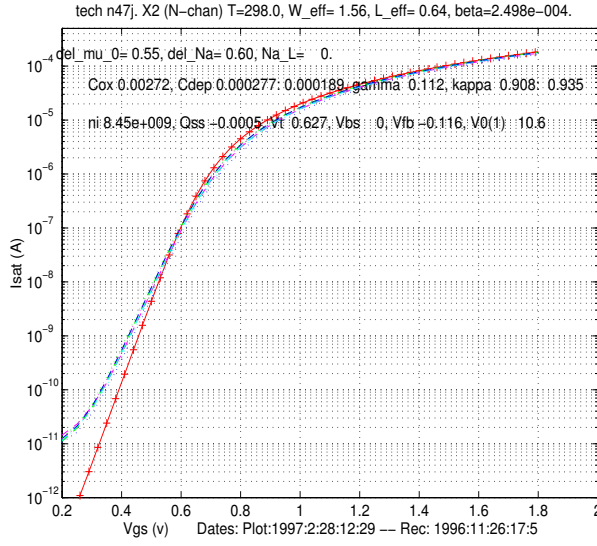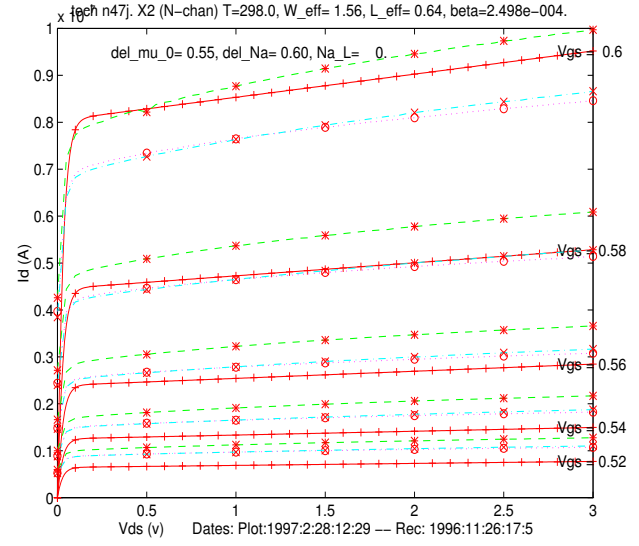Results after $\Delta\mu_0$ adjustment:

Figure 12: Model adjusted with $\Delta\mu_0$ and Measurements, P-channel $0.8um$.

Results after ΔNa adjustment:

(a)

(b)

Figure 13: Model adjusted with $\Delta\mu_0$ and ΔNa and Measurements, P-channel $0.8um$.
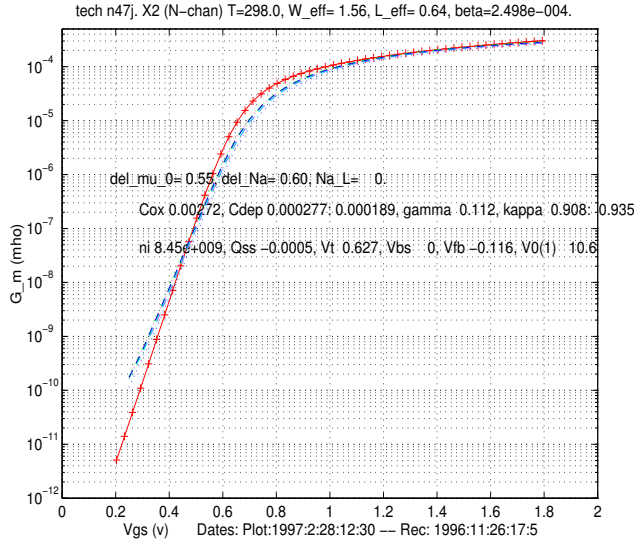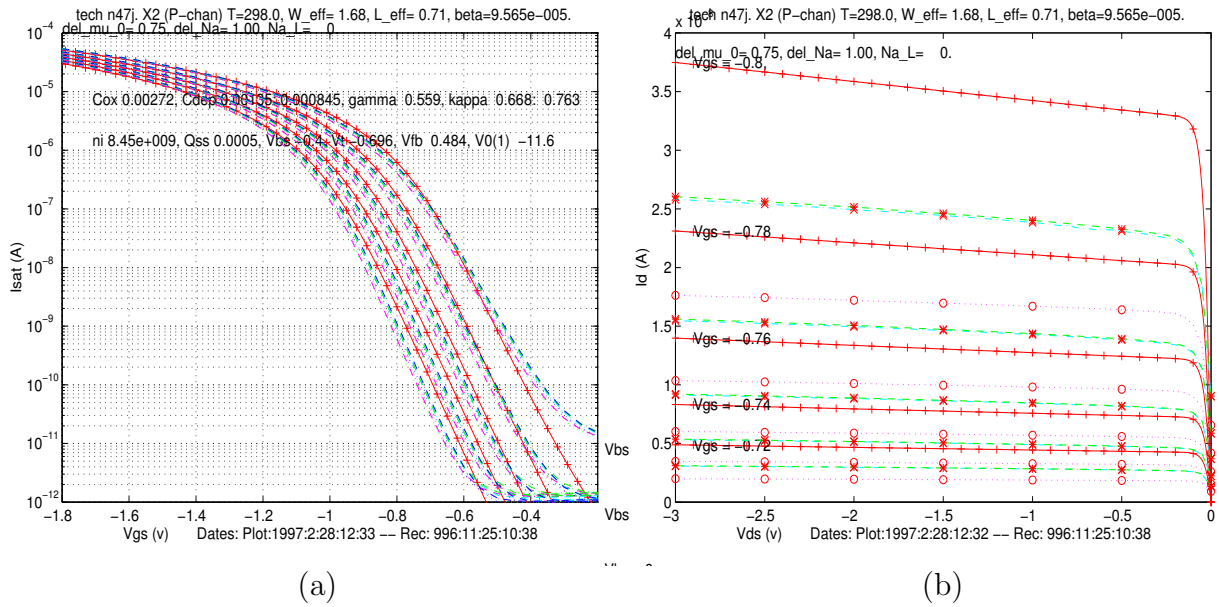
Results for g_m vs. V_{gs}:

Figure 14: g_m vs. V_{gs} Model and Measurements, P-channel $0.8um$.

6. Conclusions

This paper has developed an easy to use model suitable for circuit simulation and analysis. The model is valid for subthreshold, threshold transition, and above threshold device operation. It has a simple closed form which makes it suitable for efficient use in a circuit simulator. This has been demonstrated by its integration into the analog circuit simulator (available as freely-redistributable software for many platforms), *anaLOG.*

In addition, we worked through the derivations of the parameters used by the model. This was done in order to verify the definitions and to develop correct temperature dependencies. An important side-effect of this analysis was the discovery, previously reported in [15], that the universally used value for the intrinsic carrier concentration, 1.45×10^{10} at 300° K, is incorrect and inconsistent with its accepted theoretical definition. The correct measured value, at 300K, is 0.9976×10^{10}.

We hope that this work will clarify some aspects of device modeling for circuit analysis purposes, enhance the usefulness of the anaLOG simulator, and provide some guidance about the predictive power of models as a function of the availability of parameter values.

Appendix A: Octave (Matlab) Listing

```
function [Ids, Idssq, Idsexp] = ...
    new_parm(Vg, Vs, Vd, Vb, W, L, Tox, phi_ms, Na, Qss, mu_0, T, nsign)
% function [Ids, Idssq, Idsexp] = new_parm(Vg, Vs,...
%      Vd, Vb, W, L, Tox, phi_ms, Na, Qss, mu_0, T, nsign)
% Returns its result in uA.
% Computes MOS transistor behavior using a version of the Vittoz
% model, but based on physical parameters to derive the usual
% model parameters, beta, kappa, and Vt.
%
%     N-channel         | Vd           P-channel          | Vs
%                       |                                 |
%                  __d_|                            __s_|
%                 | |                              | |
%             g | |                            g | |
%         Vg ------| |---------Vb          Vg -----O| |--------Vb
%                 | |                              | |
%                 | |____                          | |____
%                  s |                              d |
%                    |                                |
%                    | Vs                             | Vd
%     N-well: Vb = Vsub            P-well: Vb = Vsub
%     P-well: Vb                   N-well: Vb
%
% Vg, Vs, Vd, and Vb are referred to substrate (Vb = 0 for native devices).
% Most equations use Vds, Vgs, Vbs, i.e Vs is the reference (Vs == 0).
%
% nsign indicates N or P channel device: + for N-channel, - for P-channel
%
% Results: Ids in A (i.e. x 10^6, since internal current is uA).
%          Idssq  -- square law result
%          Idsexp -- eponential law result
%          beta            Vt            Vfb
%          kappa           Vt0           Cox
%          gamma           V0            Cdep
%
%
global beta kappa Vp Vt Cox Cdep gamma Vt0 V0 Vfb Vbs phi_s ni Early_s L_0;

Vbs      = Vb - Vs;
Vdb      = Vd - Vb;

%       --------------------------------------------------
%               Physical Constants:
%       --------------------------------------------------
k      = 1.380658*10^(-23);   % Boltzmann const (Joule/deg.K) (Codata Bull. vol 63,
%                                                    pp. i-ii, 1-32)
q      = 1.60217733*10^(-19); % e-charge       (coulomb)    (Codata Bull. vol 63)
e_v    = 8.854187817e-12;     % permittivity of vacuum f/m   (Codata Bull. vol 63)
e_s    = 11.7*e_v;            % permittivity of Si    f/m   (Sze: 11.9)
e_ox   = 3.9*e_v;             % permittivity of SiO2  f/m   (Mead & Conway, M&K)
Ut     = k*T/q               %
%
%       --------------------------------------------------
%               Technology parameters:
%       --------------------------------------------------

rho    = q*Na;               % depl charge/area (Na cm^-3)
phi_ms = nsign*phi_ms;
Qss    = nsign*Qss;
Cox    = e_ox/Tox;           % F/m^2
Vfb    = phi_ms - Qss/Cox;

%       --------------------------------------------------
%               Empirical Equations:
%       --------------------------------------------------
% Temperature dependence of band gap (Eg):
% W. Bludau and A. Onton, "Temperature Dependence of the Band Gap of Silicon,"
%    J. Appl. Phy., vol.45, No. 4, April 1974, pp. 1846-1848.
% Note that they use two 2nd order polynomials and overlap the valid regions.
```

```
% They also show a Table of values of Eg from T = 0 to 300, but they do not
% state which polynomical was used in the T= 150 - 190 overlap region. While
% the numbers computed by Octave from their polynomials are close to the
% Table, they are not exact at the Table rounding to 5 digits. It appears that
% the values are closer if the second polynomial is used from T > 150. The
% differences are very small.
if(T <= 150)
  Eg = (1.1700 + 1.059e-5*T - 6.05e-7*T^2); % Bludau et. al.  for 0   < T <= 190K
else
  Eg = (1.1785 - 9.025e-5*T - 3.05e-7*T^2); % Bludau et. al.  for 150 <= T <= 300K
end;
Eg = Eg*q;
% Sproul and Green (J. Appl. Phys. vol.73 No.3 Feb 93, pp.1214-1225)
% report on actual measurements of ni from 77K to 400K. They provide
% an(other) empirical formula (which they claim fits the measurements within 1%):
% The real role of this expression is that it provides the value and temperature
% dependence of log(Na/ni), which is the only place ni is used.

ni = 1.640*10^(15)*T^(1.706)*exp(-Eg/(2*k*T));   % 9.9976e+009 at T=300 (cm^-3)
%ni = 1.45e+10
phi_f   = Ut*log(Na/ni)              % Fermi potential
phi_b   = 2*phi_f;                      % Could also be used as Tsividis-like
                                        % "pinned" value by adding a multiple of Ut.
% Temperature dependence of mu:
if(nsign > 0)
  mu      = mu_0*(T/300)^(-2.42);       % Sze pgs. 29-30.
else
  mu      = mu_0*(T/300)^(-2.30);
end;
beta      = mu*1e-4*Cox*(W/L);          % mu (cm^2/(V*s))  Cox (F/m^2)

% Channel length modulation:
Ve = nsign*Vg;
if(Ve < 0) Ve = 0; end;
lambda_c  = nsign*Early_s./(Ve + L - L_0);      % simple linear channel length
                                        % modulation (Early) effect.
                                        % From: Carver, pg 325, Fig B.3
V0     = 1./lambda_c;

gamma = (1/Cox)*sqrt(2*e_s*rho*1e6); % body effect (1e6 is cm^-3 -> m^-3)

%Vt using M&K pg. 418 plus Tsividis-like adjustment to phi_f (phi_b):
Vt     = Vfb + nsign*abs(phi_b) + nsign*gamma*sqrt(abs(phi_b) - nsign*Vbs);

% phi_s approaches zero at Vfb + Vbs and increases to asymptote
% of 2*Ut*log(Na/ni) (i.e. phi_b) for Vg above Vt.
% Sze (pg. 463-464) makes an argument about phi_s having a minimum
% and then increasing again as Vg - (Vfb + Vbs) is decreased.
% This argument is obscure, but does not matter for reasonable
% circuit values.

phi_s = phi_b*tanh((Vg - (Vfb + Vbs))./Vt);
if(phi_s < phi_b/10) phi_s = phi_b/10; end;

Cdep  = sqrt(rho*e_s*1e6./(2.0*phi_s));
kappa = Cox./(Cox + Cdep);
%    --------------------------------------------------
%               Intermediate expressions:
%      (only used due to lack of optimizer in Matlab)
%    --------------------------------------------------

k1 = 2*beta*Ut^2./kappa;
U1 = nsign/(2*Ut);
Vds = Vd - Vs;
%    --------------------------------------------------
%                   Model equations:
%    --------------------------------------------------

  If   = (log(1 + exp(U1*(kappa.*(Vg - Vt) - Vs)))).^2;
  Ir   = (log(1 + exp(U1*(kappa.*(Vg - Vt) - Vd)))).^2;
  Idsi = (If - Ir);
```

```
   Ids  = k1.*Idsi.*(1 + lambda_c.*Vds);

%      ----------------------------------------------
%            Square law and exponential results:
%      ----------------------------------------------
ifsq  = (U1*(kappa.*max(Vg - Vt, 0) - Vs)).^2;
irsq  = (U1*(kappa.*max(Vg - Vt, 0) - Vd)).^2;

Idssqi = ifsq - irsq;
Idssq  = k1.*Idssqi.*(1 + lambda_c.*Vds);

ifexp  = exp((1/Ut)*(kappa.*(Vg - Vt) - Vs));
irexp  = exp((1/Ut)*(kappa.*(Vg - Vt) - Vd));

Idsexpi = ifexp - irexp;
Idsexp = k1.*Idsexpi.*(1 + lambda_c.*Vds);
```

Appendix B: anaLOG Models and Objects

Die Temperature

```
Die Temperature                                          THERMAL

Kelvin            298.0
Celsius           25.0
Fahrenheit        77.0

Display           Kelvin
```

Physical Constants

```
Physical Constants                                       PHYSICAL

Abbreviations

C=Coulomb, F=Farad, m=meter, V=volts, f=femto, p=pico
n=nano, u=micro, m=milli, K=Kilo, M=Mega, G=Giga

Boltzmann's Constant (k) [Joules/degree]                 1.38E-23
Electron Charge (q)                                      1.602E-19C
Permittivity of Vacuum                                   8.854pF/m
Permittivity of Silicon                                  103.594pF/m
Permittivity of Silicon Dioxide                          34.531pF/m
kT/q (computed)                                          25.680mV
Silicon-Oxide Interface Charge (phi_ms)                  -0.300C

Channel-Type-Independent Fabrication Parameters
Band-gap Voltage (computed, Eg(T))[Joule-sec]            1.801E-19V
Intrinsic Carrier Concentration (computed, ni(T))[1/cm^ 3]  8.452G
```

Device Technology (N-Channel)

```
Device Technology (N-Channel)                          DEVTECHN

Process ID                                             SCN12
Lambda (identical for n-channel and p-channel)         0.600um
Wdrawn - Weff                                          490.000nm
Ldrawn - Leff                                          330.00num

Gate Oxide Thickness (Tox)                             20.00nm
Gate Capacitance (computed, Cox)                       1.727m
Carrier Mobility at T=300K [cm^ 2/(V*s)]               686.600
Carrier Mobility (computed, mu(T))                     697.805

Bulk Doping Concentration (Na) [1/cm^ 3]               3.106E16
Na Gate-Length Correction Term (NaL)                   0.000
Potential at Depletion Edge (Psi)                      0.600V
Early Effect Slope                                     0.160
Early Effect Channel Length Offset (L_0)               100.000nm

Active-to-Well Capacitance (F/um^ 2)                   0.2620f
Active-to-Gate Overlap Capacitance (F/um)              0.397f
Equivalent Linear Gate Capacitance (F/um^ 2)           0.382f
Well-to-Bulk Capacitance (F/um^ 2)                     3E-17
```

Fabrication Parameters – Adjustment Factors

```
Fabrication Parameters -- Adjustment Factors           RUNSPEC

Fabrication Run ID                  N52V

N-Channel

Na Offset (multiplicative)          1.00
Mobility Offset (multiplicative)    1.00
Qss Offset (additive)               610.000uC

P-Channel

Na Offset (multiplicative)          1.00
Mobility Offset (multiplicative)    1.00
Qss Offset (additive)               126.000uC
```

Pfet Transistor (PFET7F)

```
Pfet Transistor (PFET7F)                              PFET7F
Gate present Voltage                       5.000V
Gate Voltage on reset
Gate to Well Capacitance (computed)        50.356fF
Drain Present Voltage                      5.000V
Drain Voltage on reset
Drain to Well Capacitance (computed)       16.920fF
Source Present Voltage                     1.046uV
Source Voltage on reset
Source to Well Capacitance                 16.920fF
Well Present Voltage                       5.000V
Well Voltage on reset
Well To Substrate Capacitance (computed)   27.200fF
W (drawn, in lambda)                       28.00
L (drawn, in lambda)                       14.00
Source Area                                36.000um^ 2
Drain Area                                 36.000um^ 2
Well Area                                  100.000um^ 2
Na Offset (multiplicative)                 1.000
Mu Offset (multiplicative)                 1.000
Qss Offset (additive)                      0.000C
Vt (computed)
Kappa (computed)
```

References

[1]   E. A. Vittoz and J. Fellrath, "CMOS Analog Integrated Circuits Based on Weak Inversion Operation," *IEEE J. Solid State Circuits*, vol. SC-12, no. 3, pp. 224–231, June, 1977.

[2]   C. Mead, *Analog VLSI and Neural Systems*, Addison-Wesley, 1989, Reading, MA.

[3]   H. Oguey et S. Cserveny, "Modèle du transistor MOS valable dans un grand domaine de courants," *Bull. SEV/VSE*, Feb. 1982, , .

[4]   C. C. Enz, F. Krummenacher and E. A. Vittoz, "An Analitical MOS Transistor Model Valid in all Regions of Operation and Dedicated to Low-Voltage and Low-Current Applications," *Special Issue of the Analog Integrated Circuits and Systems Processing Journal on Low-Voltage and Low-Power Circuits*, vol. 8, pp. 83–114, 1995.

[5]   M. D. Godfrey, "CMOS Device Modeling for Subthreshold Circuits," *IEEE Transactions on Circuits and Systems II: Analog and Digital Signal Processing*, vol. 39, no. 8, pp. 532–539, August 1992.

[6]   F. J. Morin and J. P. Maita, "Electrical Properties of Silicon Containing Arsenic and Boron," *Phys. Rev.*, vol. 96, No. 1, pp. 28–35, October 1, 1954.

[7]   A. S. Grove, *Physics and Technology of Semiconductor Devices*, John Wiley & Sons, New York, 1967.

[8]   S. M. Sze, *Physics of Semiconductor Devices, 2nd ed.*, John Wiley & Sons, New York, 1981.

[9]   R. S. Muller and T. I. Kamins, *Device Electronics for Integrated Circuits, 2nd ed.*, John Wiley & Sons, New York, 1986.

[10] R. N. Hall and J. H. Racette, "Diffusion and Solubility of Copper in Extrinsic and Intrinsic Germanium, Silicon, and Gallium Arsenide," *J. Appl. Phys.*, 35, pp. 379–397, 1964.

[11] F. J. Morin and J. P. Maita, "Conductivity and Hall Effect in the Intrinsic Range of Germanium," *Phys. Rev.*, Vol. 94, No.6, pp. 1525–1529, June 15, 1954.

[12] W. Bludau and A. Onton, "Temperature Dependence of the Band Gap of Silicon," *J. Appl. Phys.*, vol. 45, No. 4, pp. 1846–1848, April 1974.

[13] A. Anselm, *Introduction to Semiconductor Theory*, MIR Publishers (English translation: Prentice-Hall, Inc., 1981), Moscow, 1978.

[14] J. R. Janesick, *Scientific Charge-Coupled Devices*, SPIE Press, 2001, Bellingham, WA.

[15] A. B. Sproul and M. A. Green, "Intrinsic Carrier Concentration and Minority-carrier Mobility of Silicon from 77 to 300K," *J. Appl. Phys.*, 73(3), pp. 1214–1225, 1 February 1993.

[16] Y. Tsividis and G. Masetti, "Problems in Precision Modelling of the MOS Transistor for Analog Applications," *IEEE Transactions on Computer-Aided Design*, CAD-3, pp. 72-79, 1984.

[17] C. C. Enz, "High Precision CMOS Micropower Amplifiers," *Thesis 802,* Ecole Polytechnique Federale de Lausanne, Lausanne, 1989.

[18] E. A. Vittoz, "The Design of High-Performance Analog Circuits on Digital CMOS Chips," *IEEE J. Solid State Circuits*, vol. SC-20, no. 3, pp. 657–665, June, 1985.

[19] E. A. Vittoz, "Analog VLSI Signal Processing: Why, Where and How?," *J. of VLSI Sig. Proc.*, vol. 8, no. 1, pp. 27–44, July 1994.

[20] E. R. Cohen and B. N. Taylor, "The 1986 Adjustment of the Fundamental Physical Constants," *Codata Bull.*, vol. 63, pp. i–ii, 1–32, Pergamon Press, November 1986.

[21] C. Mead and L. Conway, *Introduction to VLSI Systems*, Addison-Wesley, 1980, Reading, MA.

[22] A. G. Revesz, "Taxonomy of Electric Charges in Metal-Insulator-Semiconductor Systems," *Proceedings of the IEEE*, vol. 54, no. 7, pp. 1002–1003, July 1996.